

Time Series Water Wave Modeling using a Modified Euler Momentum Conservation Equation and a Momentum Equilibrium Equation

Syawaluddin Hutahaean

Ocean Engineering Program, Faculty of Civil and Environmental Engineering-Bandung Institute of Technology (ITB), Bandung 40132, Indonesia.

svawalf1@yahoo.co.id

Received: 05 Nov 2025,

Received in revised form: 03 Dec 2025,

Accepted: 08 Dec 2025,

Available online: 12 Dec 2025

©2025 The Author(s). Published by AI Publication.

This is an open-access article under the CC BY license

(<https://creativecommons.org/licenses/by/4.0/>).

Keywords— Momentum Equilibrium Equation, Hydrodynamic Force Modeling, Convective Acceleration, Wave Shoaling and Breaking, Energy Balance in Fluid Dynamics

Abstract— From an energy perspective, the water-particle velocity equations derived from the Euler or Navier Stokes momentum conservation formulations show an imbalance: kinetic energy changes occur through variations in velocity, but no corresponding source of potential energy is included. To supply this missing potential energy, a Momentum Equilibrium Equation is introduced, and its horizontal velocity is superimposed on the velocity from the momentum conservation equation. Three modifications are applied to the Euler momentum equation: reducing the driving force, applying a weighted Taylor series to the total acceleration, and treating the convective acceleration as a hydrodynamic force. Model results on a sloping bottom show that the approach can simulate shoaling and breaking effectively, pass through the breaking phase, and continue into shallow water.

I. INTRODUCTION

This study aims to develop a time-series water-wave model that more rigorously satisfies fundamental conservation laws, particularly the conservation of energy. Ensuring compliance with these principles is expected to yield a more robust wave model that more accurately represents naturally occurring wave phenomena.

Time-series water-wave modeling has a long history, beginning with the Boussinesq model (1871). Numerous subsequent studies have extended the Boussinesq framework, including work by Peregrine (1967), Hamm and Madsen (1993), Nwogu (1993), Dingemans (1997),

Johnson (1997), Madsen and Schaffer (1998), and Kirby (2003), among others.

Most Boussinesq-type equations retain the foundational structure of the Airy long-wave model, comprising two main components: (1) a water-surface elevation equation derived from the continuity equation, and (2) a horizontal water-particle velocity equation derived from Euler's momentum conservation equation. In the surface-elevation equation, changes in water level arise solely from mass flux, reflecting only the conservation of mass. If surface elevation is interpreted as potential energy, changes in elevation require an energy transfer from kinetic energy. Consequently, a surface-elevation equation derived solely from continuity lacks an explicit

energy source and therefore does not satisfy the conservation of energy. Hutahaean (2025a) addressed this issue by superposing the continuity equation with the kinetic-energy conservation equation, producing a surface-elevation formulation consistent with energy conservation.

Similarly, the velocity equation derived from Euler’s momentum conservation formulation represents a balance of forces, yet it also fails to preserve energy. Changes in velocity correspond to changes in kinetic energy, which should be supplied by variations in potential energy. Hutahaean (2025a) attempted to resolve this by formulating a pressure equation using the continuity equation; however, the resulting representation of potential-energy change remained unclear and its effect limited.

To address these limitations, the present study reformulates the momentum equilibrium to be superposed with the water-particle velocity equation. This approach provides a physically consistent potential-energy source for variations in kinetic energy while imposing continuity-based constraints on the velocity equation.

II. DEPTH AVERAGE VELOCITY, INTEGRATION AND TRANSFORMATION COEFFICIENTS

The formulation of the water-surface elevation equation and the water-particle velocity equation involves integration along the vertical-z axis. This integration can be simplified by employing the concept of depth-averaged velocity, defined as the velocity at a representative point z_0 below the still-water level (Fig. 1).

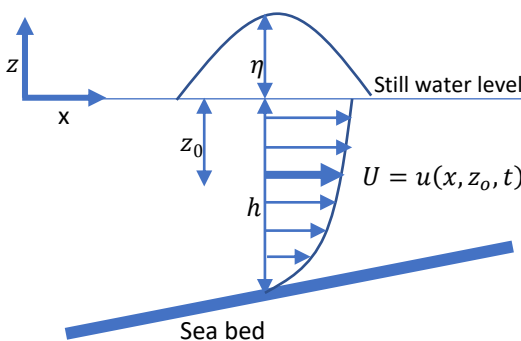


Fig (1). The concept of depth average velocity

Defined as,

$$\beta_u UD = \int_{-h}^{\eta} u dz$$

$$\beta_{uu} UUD = \int_{-h}^{\eta} uu dz$$

$$\beta_{uuu} UUU = \int_{-h}^{\eta} uuu dz$$

$$\beta_w WD = \int_{-h}^{\eta} w dz$$

$$\beta_{ww} WWD = \int_{-h}^{\eta} ww dz$$

$$\beta_{www} WWW = \int_{-h}^{\eta} www dz$$

U is the horizontal depth average velocity and W is the vertical depth average velocity, $D = h + \eta$ is the total water depth and $\beta_u, \beta_{uu}, \beta_{uuu}, \beta_w, \beta_{ww}$ and β_{www} are the integration coefficients, with values.

$$\beta_u = \frac{\sinh \theta \pi}{\theta \pi \cosh kh(1 - \varepsilon)}$$

$$\beta_{uu} = \frac{\left(\frac{1}{2} \sinh 2\theta \pi + \theta \pi\right)}{2\theta \pi \cosh^2 \theta \pi(1 - \varepsilon)}$$

$$\beta_{uuu} = \frac{\frac{1}{3} \sinh 3\theta \pi + 3 \sinh \theta \pi}{8\theta \pi \cosh^3 \theta \pi(1 - \varepsilon)}$$

$$\beta_w = \frac{\cosh \theta \pi - 1}{\theta \pi \sinh \theta \pi(1 - \varepsilon)}$$

$$\beta_{ww} = \frac{\left(\frac{1}{2} \sinh 2\theta \pi - \theta \pi\right)}{2\theta \pi \cosh^2 \theta \pi(1 - \varepsilon)}$$

$$\beta_{www} = \frac{\frac{1}{3} \cosh 3\theta \pi + 3 \cosh \theta \pi - \frac{10}{3}}{8\theta \pi \sinh^3 \theta \pi(1 - \varepsilon)}$$

The parameter θ is the deep-water coefficient, for which $\tanh \theta \pi \approx 1$ (Hutahaean, 2023). The parameter ε is a positive constant satisfying $0 < \varepsilon < 1.0$, with $z_0 = -\varepsilon h$ (Fig. 1). The formulation of the integration-coefficient equations is provided in Hutahaean (2025a).

During the integration of the conservation equations, the surface water-particle velocities u_η and w_η , also arise and must be expressed in terms of the depth-averaged velocity. This transformation is given by the following relation:

$$U = \frac{u_\eta}{\alpha_{u\eta}}$$

$$W = \frac{w_\eta}{\alpha_{w\eta}}$$

$\alpha_{u\eta}$ and $\alpha_{w\eta}$ are the transformation coefficient with the following values

$$\alpha_{u\eta} = \frac{\cosh \theta\pi}{\cosh \theta\pi(1 - \varepsilon)}$$

$$\alpha_{w\eta} = \frac{\sinh \theta\pi}{\sinh \theta\pi(1 - \varepsilon)}$$

The formulation of the transformation-coefficient equations is provided in Hutahaeen (2025a). In the following example, the integration and transformation coefficients are specified for $\theta = 0.85$, for which $\tanh \theta\pi = 0.9904608$. The procedure used to determine the value of θ is described in Section VII. The corresponding integration and transformation coefficients for this value of θ are listed in Tables (1) and (2).

Table (1) Integration Coefficient Values

ε	β_u	β_{uu}	β_{uuu}	β_w	β_{ww}
0.380	0.992	1.394	1.227	0.929	1.456
0.381	0.994	1.401	1.236	0.932	1.465
0.382	0.997	1.408	1.246	0.934	1.473
0.383	0.999	1.415	1.255	0.937	1.482
0.384	1.002	1.422	1.264	0.940	1.490
0.385	1.004	1.429	1.274	0.942	1.499
0.386	1.007	1.436	1.283	0.945	1.507
0.387	1.009	1.444	1.293	0.948	1.516
0.388	1.012	1.451	1.302	0.950	1.525
0.389	1.014	1.458	1.312	0.953	1.534
0.39	1.017	1.465	1.322	0.956	1.543

Table (2) Transformation coefficient values

ε	β_u	$\alpha_{u\eta}$	$\alpha_{w\eta}$	$ 1 - \beta_u $
0.38	1.519	2.674	2.849	0.008
0.381	1.532	2.681	2.858	0.006
0.382	1.545	2.688	2.866	0.003
0.383	1.558	2.694	2.874	0.001
0.384	1.572	2.701	2.882	0.002
0.385	1.585	2.708	2.891	0.004
0.386	1.599	2.714	2.899	0.007
0.387	1.613	2.721	2.907	0.009
0.388	1.627	2.728	2.916	0.012
0.389	1.641	2.735	2.924	0.014
0.39	1.655	2.741	2.933	0.017

The integration and transformation coefficients used in this study correspond to $\beta_u \approx 1.0$, which occurs at $\varepsilon = 0.383$. This selection is not based on a specific theoretical requirement; rather, it was chosen because it yielded favorable empirical performance.

III. WATER SURFACE ELEVATION EQUATION

As is commonly done, the water-surface elevation equation is derived from the continuity equation. However, this formulation exhibits an energy imbalance because changes in surface elevation, which represent changes in potential energy, occur without an explicit energy source. The required source should be kinetic energy. To address this issue, the kinetic-energy conservation equation is incorporated, and the continuity-based surface-elevation equation is superposed with the kinetic-energy equation as follows.

$$\frac{\partial E_{kx}}{\partial t} + \frac{\partial E_{kz}}{\partial t} = -\gamma_{x,3} \frac{\partial u E_{kx}}{\partial x} - \gamma_{z,3} \frac{\partial w E_{kz}}{\partial z}$$

This formulation differs slightly from Hutahaeen (2025a) because it includes the coefficients $\gamma_{x,3}$ and $\gamma_{z,3}$ which originate from the weighted Taylor-series approach described in Section 4.2.

$E_{kx} = \frac{uu}{2g}$ is the kinetic energy in the horizontal axis -x,

$E_{kz} = \frac{ww}{2g}$ is the kinetic horizontal in the vertical axis-z.

According to Hutahaeen (2025a), the superposition of the continuity equation and the kinetic-energy equation yields,

$$\begin{aligned}
 (\lambda_\eta + \gamma_{t,2}) \frac{\partial \eta}{\partial t} = & -\frac{\partial \beta_u UD}{\partial x} + (1 - \gamma_{x,2}) \alpha_{u\eta} U \frac{\partial \eta}{\partial x} \\
 & - \frac{1}{2g} \frac{\partial UU}{\partial t} - \frac{\beta_{ww}}{2g\beta_{uu}} \frac{\partial WW}{\partial t} \\
 & - \frac{\gamma_{x,3}}{\beta_{uu}D} \int_{-h}^{\eta} \frac{\partial u E_{kx}}{\partial x} dz \\
 & - \frac{\gamma_{z,3}}{2g\beta_{uu}D} w_\eta w_\eta w_\eta \dots (1)
 \end{aligned}$$

$$\lambda_\eta = \frac{((\beta_{uu} - \alpha_{u\eta}\alpha_{u\eta})UU + (\beta_{ww} - \alpha_{w\eta}\alpha_{w\eta})WW)}{2g\beta_u D}$$

...(2)

$\gamma_{t,2}$ and $\gamma_{x,2}$ are the weighting coefficients in the weighted Taylor series for a function $f = f(x, t)$ (Hutahaeen, 2025b). In this study, the values $\gamma_{t,2} = 1.9973$ and $\gamma_{x,2} = 0.9973$ are used. The integration of

the fifth term on the right-hand side is carried out using Leibniz's rule (Protter, Murray, Morrey, and Charles, 1985), together with the concept of depth-averaged velocity and with the assumption that the velocity at the seabed can be neglected.

$$\int_{\alpha}^{\beta} \frac{\partial f}{\partial x} dz = \frac{\partial}{\partial x} \int_{\alpha}^{\beta} u dz - f_{\beta} \frac{\partial \beta}{\partial x} + f_{\alpha} \frac{\partial \alpha}{\partial x} \quad \dots (3)$$

$$\int_{-h}^{\eta} \frac{\partial u E_{kx}}{\partial x} dz = \frac{1}{2g} \frac{\partial \beta_{uuu} U U U D}{\partial x} - \frac{u_{\eta} u_{\eta} u_{\eta}}{2g} \frac{\partial \eta}{\partial x}$$

u_{η} and w_{η} should be transformed to U and W .

3.1. Differential Vertical Velocity.

Differential water-particle velocity often arises during the formulation process. The expression for the differential vertical water-particle velocity is obtained as follows By integrating the continuity equation and applying the concept of depth-averaged velocity, we obtain:

$$w_{\eta} = -\frac{\partial \beta_u U D}{\partial x} + \alpha_{u\eta} U \frac{\partial \eta}{\partial x} \quad \dots (4)$$

Vertical depth average velocity,

$$W = \frac{1}{\alpha_{w\eta}} \left(-\frac{\partial \beta_u U D}{\partial x} + \alpha_{u\eta} U \frac{\partial \eta}{\partial x} \right)$$

$$\frac{\partial W}{\partial t} = \frac{1}{\alpha_{w\eta}} \left(-\beta_u \frac{\partial U}{\partial x} \frac{\partial \eta}{\partial t} + \left(\alpha_{u\eta} \frac{\partial \eta}{\partial x} - \beta_u \frac{\partial D}{\partial x} \right) \frac{\partial U}{\partial t} \right) \quad \dots (5)$$

The right-hand side of the 1st term of (4) is explained as,

$$w_{\eta} = -\left(\beta_u D \frac{\partial U}{\partial x} + \beta_u U \frac{\partial D}{\partial x} - \alpha_{u\eta} U \frac{\partial \eta}{\partial x} \right)$$

Differentiating with respect to the horizontal -x axis, and neglecting the second-order and cross-differential terms, we obtain:

$$\frac{\partial w_{\eta}}{\partial x} = -\left(2\beta_u \frac{\partial D}{\partial x} - \alpha_{u\eta} \frac{\partial \eta}{\partial x} \right) \frac{\partial U}{\partial x}$$

Maka,

$$\frac{\partial W}{\partial x} = -\frac{1}{\alpha_{w\eta}} \left(2\beta_u \frac{\partial D}{\partial x} - \alpha_{u\eta} \frac{\partial \eta}{\partial x} \right) \frac{\partial U}{\partial x} \quad \dots (6)$$

IV. HORIZONTAL WATER PARTICLE VELOCITY EQUATION

The horizontal water-particle velocity equation is formulated using a modified form of Euler's momentum conservation equation. In this study, three modifications were applied to the original formulation.

4.1. Original Euler's momentum conservation equation.

Euler's momentum conservation principles on the (x, z) plane consist of two components: the horizontal momentum equation in the x direction and the vertical momentum equation in the z direction. These are expressed as:

$$\frac{\partial u}{\partial t} + u \frac{\partial u}{\partial x} + w \frac{\partial u}{\partial z} = -\frac{1}{\rho} \frac{\partial p}{\partial x}$$

$$\frac{\partial w}{\partial t} + u \frac{\partial w}{\partial x} + w \frac{\partial w}{\partial z} = -\frac{1}{\rho} \frac{\partial p}{\partial z} - g$$

u is the horizontal water particle velocity, w is the vertical water particle velocity, p is the pressure, ρ is the water mass density, g is the gravity, x is the horizontal axis, z is the vertical axis and t is the time, see Fig (2).

As illustrated in Fig. 2, the acceleration terms on the left-hand side, interpreted through a Taylor series expansion, represent the differences in velocity between points E and F in both the horizontal and vertical directions. The driving forces on the right-hand side correspond to pressure differences: the horizontal pressure gradient arises from the difference between pressures at points A and B, while the vertical pressure gradient reflects the pressure difference between points C and D. Because the pressure field is obtained by integrating the vertical momentum equation, this integration yields the pressure distribution as well as the maximum pressure difference (i.e., the driving force) acting within the fluid.

The magnitude of the resulting driving force renders this equation inappropriate for representing short, large-amplitude waves. Although it can be applied to long waves of small amplitude, it still produces nonphysical behavior, particularly a wave height that increases without bound. The detailed analysis underlying this conclusion is not included here for brevity, and an exhaustive treatment of Euler's momentum conservation equation falls outside the present scope.

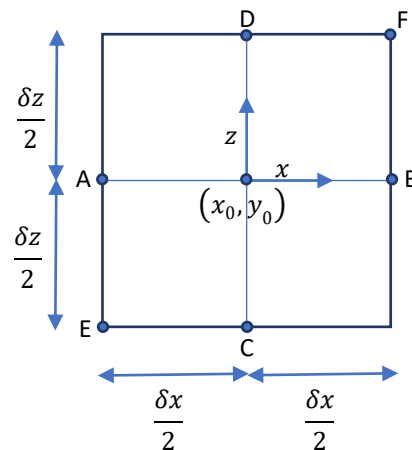


Fig (2). Control volume in the Euler's equation.

For practical reference, this Euler-based formulation is termed the unstable equilibrium equation. Its intrinsic instability provides the conceptual foundation for formulating alternative versions of unstable equilibrium equations.

4.2. Modified Euler’s momentum conservation equation.

The original Euler momentum equation is modified in three ways: (1) the driving force is reduced by shortening the separation between the velocity-difference observation points; (2) a weighted Taylor expansion is applied; and (3) the convective acceleration term is treated as a hydrodynamic force.

a. Modification 1

As previously explained, widely spaced velocity-difference points produce an excessively large driving force, leading to numerical instability, particularly in short-wave simulations. To mitigate this, the distance between the horizontal and vertical velocity-difference observation points is reduced (Fig. 3).

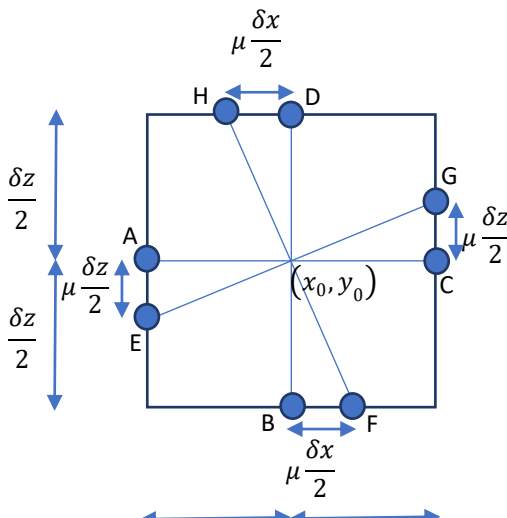


Fig (3) Control volume and control points for the modified Euler equation

The horizontal velocity difference is evaluated between points E and G, and the vertical velocity difference between points F and H. These shortened separations reduce the driving force compared with the original Euler formulation. The momentum equations become:

$$\frac{\partial u}{\partial t} + u \frac{\partial u}{\partial x} + \mu w \frac{\partial u}{\partial z} = -\frac{1}{\rho} \frac{\partial p}{\partial x}$$

$$\frac{\partial w}{\partial t} - \mu u \frac{\partial w}{\partial x} + w \frac{\partial w}{\partial z} = -\frac{1}{\rho} \frac{\partial p}{\partial z} - g$$

Using irrotational-flow properties, these can be written as:

$$\frac{\partial u}{\partial t} + \frac{1}{2} \frac{\partial}{\partial x} (uu + \mu ww) = -\frac{1}{\rho} \frac{\partial p}{\partial x}$$

$$\frac{\partial w}{\partial t} + \frac{1}{2} \frac{\partial}{\partial z} (-\mu uu + ww) = -\frac{1}{\rho} \frac{\partial p}{\partial z} - g$$

This formulation may be regarded as an unstable equilibrium equation, as the points defining the driving force differ from those defining the velocity gradients. The coefficient μ is a positive parameter within $0 \leq \mu \leq 1$, and its effects are examined in Section VII.

b. Modification 2

The total variation of a function $f = f(x, z, t)$ using a first-order truncated weighted Taylor series based on the equation of Hutahaean (2025b) is as follows.

$$\delta f = \gamma_{t,3} \delta t \frac{\partial f}{\partial t} + \frac{\gamma_{x,3}}{2} \delta x \frac{\partial f}{\partial x} + \frac{\gamma_{z,3}}{2} \delta z \frac{\partial f}{\partial z}$$

$\gamma_{t,3}$, $\gamma_{x,3}$ and $\gamma_{z,3}$ is the weighting coefficient t weighted Taylor series for function $f = f(x, z, t)$, with value $\gamma_{t,3} = 3.04933$, $\gamma_{x,3} = \gamma_{z,3} = 2.04933$, Hutahaean (2025b).

Applying this weighted Taylor expansion to the modified Euler momentum equation yields,

$$\gamma_{t,3} \frac{\partial u}{\partial t} + \frac{\gamma_{x,3}}{2} \frac{\partial}{\partial x} (uu + \mu ww) = -\frac{1}{\rho} \frac{\partial p}{\partial x}$$

$$\gamma_{t,3} \frac{\partial w}{\partial t} + \frac{\gamma_{z,3}}{2} \frac{\partial}{\partial z} (-\mu uu + ww) = -\frac{1}{\rho} \frac{\partial p}{\partial z} - g$$

The purpose of the weighted Taylor series is to produce shorter modeled wavelengths that better match natural wavelengths, while simultaneously reducing the driving force and water-particle velocities.

c. Modification 3

The third modification interprets the convective acceleration in the second term on the left-hand side as a hydrodynamic force directed from higher to lower energy. Consequently, this term is assigned a negative sign (-), Hutahaean (2025c).

$$\gamma_{t,3} \frac{\partial u}{\partial t} - \frac{\gamma_{x,3}}{2} \frac{\partial}{\partial x} (uu + \mu ww) = -\frac{1}{\rho} \frac{\partial p}{\partial x} \quad \dots (7)$$

$$\gamma_{t,3} \frac{\partial w}{\partial t} - \frac{\gamma_{z,3}}{2} \frac{\partial}{\partial z} (-\mu uu + ww) = -\frac{1}{\rho} \frac{\partial p}{\partial z} - g \quad \dots (8)$$

4.3. Pressure and Driving-Force Equations.

The pressure and driving-force expressions are obtained by integrating Eq. (8) with respect to the vertical coordinate -z.

To ensure that velocity changes comply with the continuity equation, the term $\frac{\partial w}{\partial t}$ in equation (8) is replaced with the vertically integrated continuity relation.

Following Hutahaean (2025a), the resulting pressure equation is:

$$\begin{aligned} \frac{\gamma_{z,3}}{\rho} p &= \gamma_{t,3} \int_z^\eta \left(\frac{\partial}{\partial t} \int_z^\eta \frac{\partial u}{\partial x} dz \right) dz + \frac{\partial w_\eta}{\partial t} (\eta - z) \\ &\quad - \frac{\gamma_{z,3}}{2} (-\mu u_\eta u_\eta + w_\eta w_\eta) \\ &\quad + \frac{\gamma_{z,3}}{2} (-\mu u u + w w) + g(\eta - z) \end{aligned}$$

Hence, the horizontal driving-force equation is,

$$\begin{aligned} \frac{\gamma_{z,3}}{\rho} \frac{\partial p}{\partial x} &= \gamma_{t,3} \frac{\partial}{\partial x} \int_z^\eta \left(\frac{\partial}{\partial t} \int_z^\eta \frac{\partial u}{\partial x} dz \right) dz \\ &\quad + \gamma_{t,3} \frac{\partial w_\eta}{\partial t} \frac{\partial \eta}{\partial x} \\ &\quad - \frac{\gamma_{z,3}}{2} \frac{\partial}{\partial x} (-\mu u_\eta u_\eta + w_\eta w_\eta) \\ &\quad + \frac{\gamma_{z,3}}{2} \frac{\partial}{\partial x} (-\mu u u + w w) + g \frac{\partial \eta}{\partial x} \quad \dots (9) \end{aligned}$$

Integration of the first term on the right-hand side, solved using the velocity potential equation, Hutahaean (2025a), obtains

$$\begin{aligned} \frac{\partial}{\partial x} \int_z^\eta \left(\frac{\partial}{\partial t} \int_z^\eta \frac{\partial u}{\partial x} dz \right) dz &= - \frac{\partial w_\eta}{\partial t} \frac{\partial \eta}{\partial x} \\ &\quad + \left(\frac{\partial u_\eta}{\partial t} - \frac{\partial u}{\partial t} \right) \end{aligned}$$

Substituted to (7),

$$\begin{aligned} \frac{\gamma_{z,3}}{\rho} \frac{\partial p}{\partial x} &= \gamma_{t,3} \left(- \frac{\partial w_\eta}{\partial t} \frac{\partial \eta}{\partial x} + \left(\frac{\partial u_\eta}{\partial t} - \frac{\partial u}{\partial t} \right) \right) \\ &\quad + \gamma_{t,3} \frac{\partial w_\eta}{\partial t} \frac{\partial \eta}{\partial x} \\ &\quad - \frac{\gamma_{z,3}}{2} \frac{\partial}{\partial x} (-\mu u_\eta u_\eta + w_\eta w_\eta) \\ &\quad + \frac{\gamma_{z,3}}{2} \frac{\partial}{\partial x} (-\mu u u + w w) + g \frac{\partial \eta}{\partial x} \end{aligned}$$

The first and third terms on the right-hand side cancel one another, and it is important to recall that $\gamma_{z,3} = \gamma_{x,3}$,

$$\begin{aligned} \frac{\gamma_{x,3}}{\rho} \frac{\partial p}{\partial x} &= \gamma_{t,3} \left(\frac{\partial u_\eta}{\partial t} - \frac{\partial u}{\partial t} \right) \\ &\quad - \frac{\gamma_{z,3}}{2} \frac{\partial}{\partial x} (-\mu u_\eta u_\eta + w_\eta w_\eta) \\ &\quad + \frac{\gamma_{z,3}}{2} \frac{\partial}{\partial x} (-\mu u u + w w) \\ &\quad + g \frac{\partial \eta}{\partial x} \quad \dots (10) \end{aligned}$$

4.4. Horizontal Velocity Equation.

Substituting Eq. (10) into Eq. (7) gives:

$$\begin{aligned} \gamma_{t,3} \frac{\partial u}{\partial t} - \frac{\gamma_{x,3}}{2} \frac{\partial}{\partial x} (u u + \mu w w) &= -\gamma_{t,3} \left(\frac{\partial u_\eta}{\partial t} - \frac{\partial u}{\partial t} \right) \\ &\quad + \frac{\gamma_{z,3}}{2} \frac{\partial}{\partial x} (-\mu u_\eta u_\eta + w_\eta w_\eta) \end{aligned}$$

$$- \frac{\gamma_{z,3}}{2} \frac{\partial}{\partial x} (-\mu u u + w w) - g \frac{\partial \eta}{\partial x}$$

At $z = \eta$,

$$\gamma_{t,3} \frac{\partial u_\eta}{\partial t} - \frac{\gamma_{x,3}}{2} \frac{\partial}{\partial x} (u_\eta u_\eta + \mu w_\eta w_\eta) = -g \frac{\partial \eta}{\partial x}$$

Transformed into depth average velocity equation,

$$\begin{aligned} \gamma_{t,3} \alpha_{u\eta} \frac{\partial U}{\partial t} - \frac{\gamma_{x,3}}{2} \frac{\partial}{\partial x} (\alpha_{u\eta} \alpha_{u\eta} U U + \mu w_\eta w_\eta) &= \\ -g \frac{\partial \eta}{\partial x} \quad (11) \end{aligned}$$

w_η does not need to be transformed to the depth average velocity.

Equation (11) represents the final governing equation for the depth-averaged horizontal water-particle velocity. The left-hand side includes the kinetic-energy variation term $\frac{\partial U}{\partial t}$, which, in principle, should be supplied by changes in potential energy. This requires a contribution from $\frac{\partial \eta}{\partial t}$. It appears implicitly in w_η , but only through its horizontal derivative to the axis- x $\frac{\partial \mu_z w_\eta w_\eta}{\partial x}$. Consequently, the transfer of potential-energy variation to kinetic-energy variation is minimal.

To obtain an adequate contribution from $\frac{\partial \eta}{\partial t}$, equation. (11) is superposed with the momentum-equilibrium equation.

V. MOMENTUM EQUILIBRIUM EQUATION

5.1. Conservation of Mass.

The momentum equilibrium equation is derived using the conservation of mass, analogous to the standard continuity equation. The derivation assumes that over a sufficiently small-time interval δt from $t = t - \frac{\delta t}{2}$ ke $t = t + \frac{\delta t}{2}$, the inflow and outflow velocities within the control volume can be represented by the velocity at $t = t$, obtaining the following mass conservation equation,

$$\frac{\delta u}{\delta x} + \frac{\delta w}{\delta z} = 0 \quad \dots (12)$$

This form applies to incompressible flow within a fixed control volume. The full derivation is not reproduced here, as it is standard and can be found in Dean (1991).

5.2. Momentum equilibrium equation.

Taking δx and δz close to zero (10) yields the continuity equation,

$$\frac{\partial u}{\partial x} + \frac{\partial w}{\partial z} = 0 \quad \dots (13)$$

The same relation can be obtained using an alternative approach in which the velocity defines δu and δw using a weighted Taylor series.

$$\delta u = \gamma_{t,3} \delta t \frac{\partial u}{\partial t} + \gamma_{x,3} \delta x \frac{\partial u}{\partial x} + \gamma_{z,3} \mu \delta z \frac{\partial u}{\partial z}$$

$$\delta w = \gamma_{t,3} \delta t \frac{\partial w}{\partial t} - \gamma_{x,3} \mu \delta x \frac{\partial w}{\partial x} + \gamma_{z,3} \delta z \frac{\partial w}{\partial z}$$

Substituting these expressions into the mass-conservation equation gives:

$$\frac{\gamma_{t,3} \delta t \frac{\partial u}{\partial t} + \gamma_{x,3} \delta x \frac{\partial u}{\partial x} + \gamma_{z,3} \mu \delta z \frac{\partial u}{\partial z}}{\delta x} + \frac{\gamma_{t,3} \delta t \frac{\partial w}{\partial t} - \gamma_{x,3} \mu \delta x \frac{\partial w}{\partial x} + \gamma_{z,3} \delta z \frac{\partial w}{\partial z}}{\delta z} = 0 \dots (14)$$

If, over small-time interval $t = t - \frac{\delta t}{2}$ ke $t = t + \frac{\delta t}{2}$ the velocity is approximated as constant $t = t$, hence $\frac{\partial u}{\partial t} = \frac{\partial w}{\partial t} = 0$, as written in the conservation of mass equation. If

$\mu = 0$, the continuity equation is,

$$\frac{\partial u}{\partial x} + \frac{\partial w}{\partial z} = 0$$

When temporal variations are retained at interval $t = t - \frac{\delta t}{2}$ to $t = t + \frac{\delta t}{2}$, equation $\delta x = \delta z$ and (14) are multiplied by δx to obtain,

$$\gamma_{t,3} \delta t \frac{\partial u}{\partial t} + \gamma_{x,3} \delta x \frac{\partial u}{\partial x} + \gamma_{z,3} \mu \delta z \frac{\partial u}{\partial z} + \gamma_{t,3} \delta t \frac{\partial w}{\partial t} - \gamma_{x,3} \mu \delta x \frac{\partial w}{\partial x} + \gamma_{z,3} \delta z \frac{\partial w}{\partial z} = 0$$

Dividing by δt close to zero, where $\frac{\delta x}{\delta t} = u$ and $\frac{\delta z}{\delta t} = w$ and using the irrotationality condition $\frac{\partial u}{\partial z} = \frac{\partial w}{\partial x}$,

$$\gamma_{t,3} \frac{\partial u}{\partial t} + \frac{\gamma_{x,3}}{2} \frac{\partial}{\partial x} (uu + \mu ww) + \gamma_{t,3} \frac{\partial w}{\partial t} + \frac{\gamma_{x,3}}{2} \frac{\partial}{\partial z} (-\mu uu + ww) = 0$$

The second and fourth terms correspond to convective acceleration. As argued by Hutahaean (2025c), these represent hydrodynamic forces directed from higher to lower energy and therefore must carry a negative sign. This leads to the momentum equilibrium equation:

$$\gamma_{t,3} \frac{\partial u}{\partial t} - \frac{\gamma_{x,3}}{2} \frac{\partial}{\partial x} (uu + \mu ww) + \gamma_{t,3} \frac{\partial w}{\partial t} - \frac{\gamma_{x,3}}{2} \frac{\partial}{\partial z} (-\mu uu + ww) = 0 \dots (15)$$

5.3. Integration of momentum equilibrium equation

Equation (15) is rewritten into an equation for the horizontal water-particle velocity and integrated with respect to the vertical-z axis.

$$\gamma_{t,3} \int_{-h}^{\eta} \frac{\partial u}{\partial t} dz = \frac{\gamma_{x,3}}{2} \int_{-h}^{\eta} \frac{\partial (uu + \mu ww)}{\partial x} dz$$

$$-\gamma_{t,3} \int_{-h}^{\eta} \frac{\partial w}{\partial t} dz + \frac{\gamma_{z,3}}{2} (-\mu u_{\eta} u_{\eta} + w_{\eta} w_{\eta}) \quad (16)$$

where the seabed vertical water-particle velocities u_{-h} and w_{-h} are neglected.

The integration is carried out using Leibniz's rule (Protter, Murray, Morrey, & Charles, 1985), together with the concept of depth-averaged velocity, and recognizing that the still-water depth is constant in time t , where $\frac{\partial h}{\partial t} = 0$,

$$\int_{-h}^{\eta} \frac{\partial u}{\partial t} dz = \beta_u D \frac{\partial U}{\partial t} + (\beta_u - \alpha_{u\eta}) U \frac{\partial \eta}{\partial t}$$

$$\int_{-h}^{\eta} \frac{\partial w}{\partial t} dz = \beta_w H \frac{\partial W}{\partial t} + (\beta_w - \alpha_{w\eta}) W \frac{\partial \eta}{\partial t}$$

In this integration, the seabed horizontal water-particle velocities u_{-h} and w_{-h} are neglected. The equation for $\frac{\partial w}{\partial t}$ is equation (5).

Substituting the expressions $\int_{-h}^{\eta} \frac{\partial u}{\partial t} dz$, $\int_{-h}^{\eta} \frac{\partial w}{\partial t} dz$ and $\frac{\partial w}{\partial t}$ to equation (15),

$$\lambda_u = \left(\beta_u - \frac{\beta_w}{\alpha_{w\eta}} \left(\beta_u \frac{\partial D}{\partial x} - \alpha_{u\eta} \frac{\partial \eta}{\partial x} \right) \right)$$

$$\lambda_u \frac{\partial U}{\partial t} = - \frac{(\beta_u - \alpha_{u\eta})}{H} U \frac{\partial \eta}{\partial t} - \frac{(\beta_w - \alpha_{w\eta})}{H} W \frac{\partial \eta}{\partial t}$$

$$+ \frac{\beta_w \beta_u}{\alpha_{w\eta}} \frac{\partial U}{\partial x} \frac{\partial \eta}{\partial t} + \frac{\gamma_{x,3}}{2 \gamma_{t,3} D} \int_{-h}^{\eta} \frac{\partial (uu + \mu ww)}{\partial x} dz$$

$$+ \frac{\gamma_{z,3}}{2 \gamma_{t,3} D} (-\mu u_{\eta} u_{\eta} + w_{\eta} w_{\eta}) \dots (17)$$

This equation shows the contribution of $\frac{\partial \eta}{\partial t}$ both directly and through w_{η} towards changes in $U = \frac{\partial U}{\partial t}$. Using Leibniz integration and the concept of depth-averaged velocity, the expressions for $\int_{-h}^{\eta} \frac{\partial uu}{\partial x} dz$ and $\int_{-h}^{\eta} \frac{\partial ww}{\partial x} dz$ is.

$$\int_{-h}^{\eta} \frac{\partial uu}{\partial x} dz = \frac{\partial \beta_{uu} UUD}{\partial x} - u_{\eta} u_{\eta} \frac{\partial \eta}{\partial x} - u_{-h} u_{-h} \frac{\partial h}{\partial x}$$

Seabed velocity is neglected, and the first term on the right-hand side is expanded.

The surface horizontal velocity u_{η} is transformed into the depth-averaged velocity U

$$\int_{-h}^{\eta} \frac{\partial uu}{\partial x} dz = \beta_{uu} \left(UU \frac{\partial D}{\partial x} + 2UD \frac{\partial U}{\partial x} \right) - \alpha_{u\eta} \alpha_{u\eta} UU \frac{\partial \eta}{\partial x}$$

$$\int_{-h}^{\eta} \frac{\partial ww}{\partial x} dz = \frac{\partial \beta_{ww} WWD}{\partial x} - w_{\eta} w_{\eta} \frac{\partial \eta}{\partial x} - w_{-h} w_{-h} \frac{\partial h}{\partial x}$$

Seabed velocity is neglected, and the first term on the right-hand side is expanded,

$$\int_{-h}^{\eta} \frac{\partial ww}{\partial x} dz = \beta_{ww} \left(WW \frac{\partial D}{\partial x} + 2WD \frac{\partial W}{\partial x} \right) - w_{\eta} w_{\eta} \frac{\partial \eta}{\partial x}$$

5.4. Final equation for the horizontal depth-averaged velocity.

In equation (16), the first, second, and third terms on the right-hand side explicitly contain $\frac{\partial \eta}{\partial t}$, and the fifth term, through the kinematic free surface boundary condition, also contains $\frac{\partial \eta}{\partial t}$. Therefore, this equation contains many sources of energy contributing to the change of kinetic energy on the left-hand side. However, this equation cannot stand alone because it does not have a driving force. By superposing equation (11) with equation (17), a new horizontal depth-averaged water particle velocity equation is obtained that includes sufficient potential energy sources to support the kinetic energy changes in $\frac{\partial U}{\partial t}$. The superposition is performed simply by adding the two equations, and the result is:

$$\begin{aligned}
 (\gamma_{t,3}\alpha_{u\eta} + \lambda_u) \frac{\partial U}{\partial t} &= \frac{\gamma_{x,3}}{2} \frac{\partial}{\partial x} (\alpha_{u\eta}\alpha_{u\eta}UU + \mu_z w_\eta w_\eta) \\
 &\quad - g \frac{\partial \eta}{\partial x} \\
 &\quad - \frac{(\beta_u - \alpha_{u\eta})}{H} U \frac{\partial \eta}{\partial t} \\
 &\quad - \frac{(\beta_w - \alpha_{w\eta})}{H} W \frac{\partial \eta}{\partial t} \\
 &\quad + \frac{\beta_w \beta_u}{\alpha_{w\eta}} \frac{\partial U}{\partial x} \frac{\partial \eta}{\partial t} \\
 &\quad + \frac{\gamma_{x,3}}{2\gamma_{t,3}D} \int_{-h}^{\eta} \frac{\partial (uu + \mu ww)}{\partial x} dz \\
 &\quad + \frac{\gamma_{z,3}}{2\gamma_{t,3}D} (-\mu u_\eta u_\eta + w_\eta w_\eta) \quad \dots (18)
 \end{aligned}$$

VI. NUMERICAL METHOD

The Finite Difference Method is used for spatial differentiation, while the time differentiation is solved using a predictor–corrector method. In the predictor stage, the Finite Difference Method with a central difference scheme is applied, and in the corrector stage, an integration method based on Newton–Cotes numerical integration is used. Details of the predictor–corrector method can be found in Hutahaean (2024). The formulation of the following equations can be found in Hutahaean (2025c).

a. Time-step δt .

$$-\frac{\delta t^2}{6} \sigma^2 + \frac{\delta t}{2} \sigma - \varepsilon = 0 \quad \dots (19)$$

b. Grid-size δx .

$$\delta x = 3.1 \frac{\sigma}{k} \delta t \quad \dots (20)$$

ε is a very small number. In this research $\varepsilon = 0.005$. Smaller ε is followed by smaller time step δt , and the better the accuracy.

c. Wave number calculation

Estimated deep water number,

$$k_0 = 0.5 \gamma_{t,2} \gamma_{t,3} \frac{\sigma^2}{g}$$

$$h_0 = 0.5 L_0 = \frac{\pi}{k_0}$$

Wave number at shallow water $h < h_0$,

$$k = \frac{k_0 h_0}{h}$$

VII. RESEARCH ON THE MODEL

7.1. Wave profile input.

The model is executed with an input solitary wave. In this study the solitary wave is interpreted only as a wave profile in which the wave crest and wave trough are above the still water level. With this profile the initial condition at the input point is satisfied, namely $\eta(0,0) = \frac{\partial \eta}{\partial t} = 0$.

The input wave equation is,

$$\eta(0,t) = -A \cos \sigma t + A \quad \dots (21)$$

and the wave profile is shown in Fig. 4. The wave amplitude used is $A = 1.2 \text{ m}$ and the wave period $T = 8.0 \text{ sec}$.

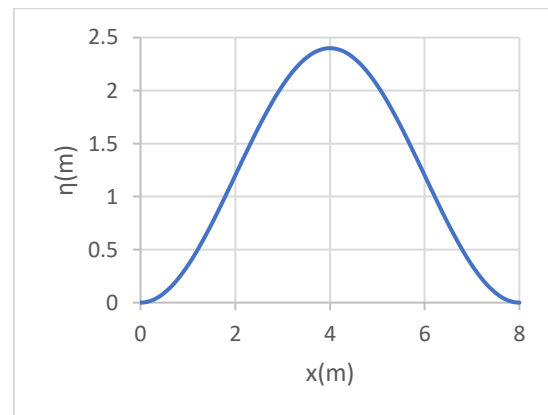


Fig (4) Wave input on t.

7.2. Study on flat bottom

The purpose of this section is to determine the appropriate value of one of the model coefficients, namely the deep-water coefficient θ .

7.2.1. Study of the deep-water coefficient θ .

Each wave period has its own value of the deep-water coefficient θ , although the differences are small. Therefore, a single value of θ can be used for all wave periods, especially for relatively small wave periods. The following is an example of a study of θ , using a wave with period 8.0 seconds and deep-water wave amplitude $A_0 = 1.2 \text{ m}$,

The model is executed using $\theta = 0.70$ and $\mu = 0$, with a simulation time of 10 wave periods or 80 seconds. The model results are presented in Fig. (5) and Fig. (6). In these figures, the crest line is the line connecting the wave crests. For a wave over a flat bottom, the crest line should remain constant at $\eta = 2A = 2.40 \text{ m}$. In Fig. (5), it can be seen that the crest line increases, indicating a growth of wave height. This occurs because the value of θ is too small.

At the tail region, small ripples are generated. The amplitude of these ripples is determined by the wave steepness. The greater the wave steepness, the larger the ripples. These ripples can be reduced by decreasing the wave amplitude, or by reducing the value of θ , although they cannot be fully eliminated.

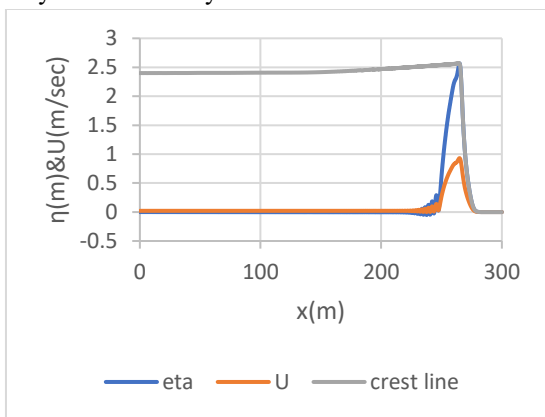
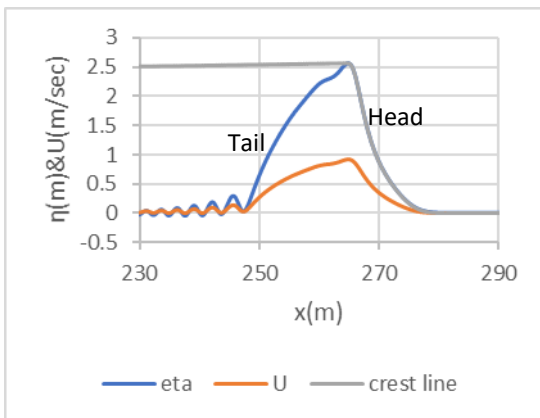


Fig (5). Results of model, $\theta = 0.70$ and $\mu = 0$



In Fig. (7) the model results for $\theta = 1.2$, are shown.

According to velocity potential theory, a larger θ is considered better because $\tanh \theta \pi$ approaches one, Hutahaean (2023). However, for this time-series model this property does not hold. The wave height decreases and the wave ripples become larger.

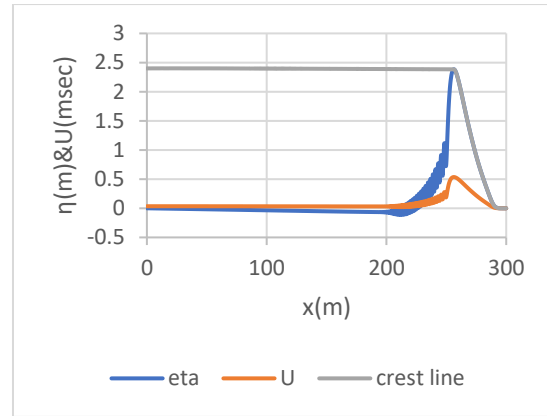


Fig (7). Model results $\theta = 1.2$ and $\mu = 0$

Thus, the optimal value of θ is the smallest value for which no increase in wave height occurs. For the wave period of 8 seconds, the optimal value is $\theta = 0.81$. The model results are shown in Fig. (8).

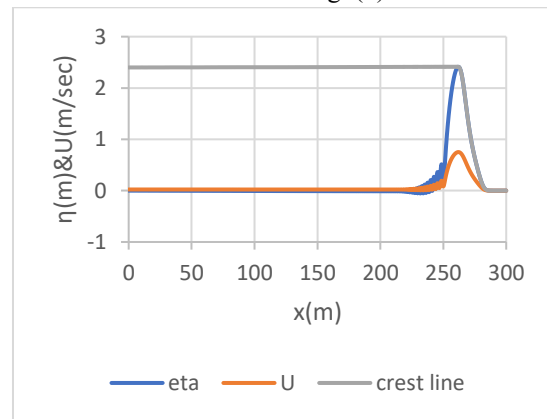


Fig (8). Model results, $\theta = 0.81$ and $\mu = 0$

7.2.2. Study of the coefficient μ on flat bottom.

The model is executed using $\theta = 0.81$ and $\mu = 0.01$ with a uniform distribution of μ over the entire domain. A wave amplitude of 1.2 m and a wave period of 8.0 seconds are used. The model results are shown in Fig. (9). A reduction in wave height is observed, and the larger the value of μ , the greater the reduction.

The reduction of wave height represents a loss of wave energy. Therefore, the coefficient μ can be interpreted as the resultant of all energy losses, including viscosity, radiation stress, bottom friction, and other mechanisms. The larger the value of μ , the greater the amount of energy lost. For flat-bottom conditions, it is appropriate to use $\mu = 0$, although a value $\mu > 0$ may be used when energy losses need to be taken into account.

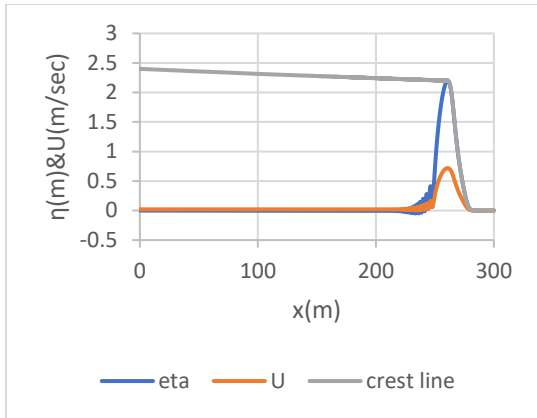


Fig (9). Model results, $\theta = 0.81, A_0 = 1.2 \text{ m}$ and $\mu = 0.01$

7.2.3. Wave energy losses equation.

It has been shown that μ is an energy loss coefficient. The magnitude of the energy loss depends on the magnitude of the energy itself, so the value of μ is also determined by the amount of energy. Hence μ is a function of wave energy. Wave energy at a given point changes with time, and wave energy also changes from one point to another. Therefore, the energy loss coefficient μ is a function of space and time, $\mu = \mu(x, t)$, with the following form of equation:

$$\mu(x, t) = c_\mu \sigma^2 \frac{u_\eta u_\eta + w_\eta w_\eta}{2g} \left(1 + 2 \left(\frac{\partial \eta}{\partial x} \right)^2 \right) \frac{\pi}{h + \eta} \dots (22)$$

$$c_\mu = 0.21 \text{ m}^{-1} \text{ sec}^4$$

This equation is formulated intuitively and through trial and error, without using conservation laws or equilibrium laws. A discussion of the equation will be presented in the next paper. The coefficient c_μ is obtained through trial and error by to match the breaking wave height from Komar and Gaughan (1972), equation (23). The value of c_μ varies slightly with wave period, with an average value of 0.21. Therefore $c_\mu = 0.21$ is used.

It should be noted that the average value $c_\mu = 0.21$ is the result of fitting the breaking wave height H_b to the breaking wave height from equation (23), H_{b-KG} . Using a breaking wave height from other researchers would result in a different value of c_μ .

The breaking wave height equation from Komar and Gaughan (1972) is,

$$H_{b-KG} = 0.39 g^{1/5} (T_0 H_0^2)^{2/5} \dots (23)$$

7.3. Model Results on a Sloping Bottom.

The model was executed over a sloping bottom with a slope of 0.05 for several wave periods. The deep-water depth is denoted as h_0 , calculated using the equation

presented in Section VI, where the value of h_0 varies according to the wave period T . In the shallow-water region, a constant water depth of 1.0 m was used. Consequently, the domain length also varies depending on the wave period.

The wave-breaking parameters are presented in Table (3), while the shoaling, breaking, and wave profiles in shallow water for several wave periods are shown in Figures (11–19)

Table (3). Parameter breaking output model.

T (sec)	H_0 (m)	H_b (m)	h_b (m)	$\frac{H_b}{h_b}$	H_{b-KG} (m)
7.0	0.85	2.068	5.226	0.396	2.050
8.0	1.20	2.843	7.452	0.381	2.85
9.0	1.45	3.491	8.932	0.391	3.475
10.0	1.85	4.410	11.469	0.384	4.405
11.0	2.15	5.196	13.276	0.391	5.161
12.0	2.55	6.172	15.768	0.391	6.125

In Table (3), H_0 represents the deep-water wave height, H_b is the breaking wave height, and h_b is the breaking water depth. It can be seen that the modeled breaking wave height H_b is fairly close to the Komar–Gaughan (1972) breaker height H_{b-KG} . The breaker depth index $\frac{H_b}{h_b}$ is much lower than the McCowan (1894) criterion, which states $\frac{H_b}{h_b} = 0.78$. However, under the McCowan (1894) criterion, waves reach the coastline with relatively large wave heights.

Figures (10–18) present the shoaling–breaking patterns and wave profiles at the breaking point and in shallow water for several wave periods. The breaking wave height corresponds to the highest point along the crest line, which is the line connecting the wave crests.

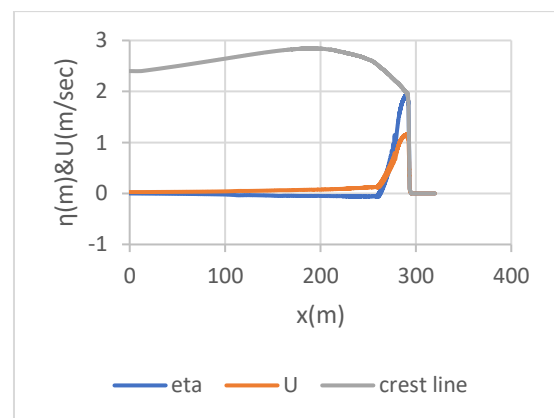


Fig (10) Shoaling-breaking, wave period 8.0 sec.

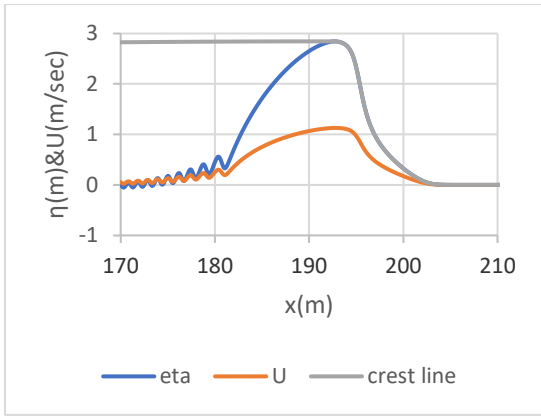


Fig (11) Wave profile around the breaking point $h_b = 7.452\text{ m}$, wave period 8.0 sec.

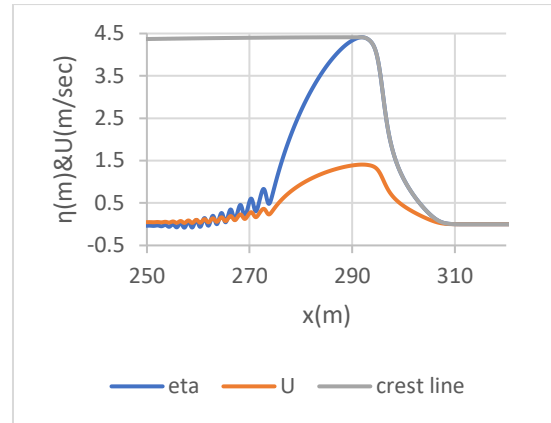


Fig (14) Wave profile around breaking point $h_b = 11.469\text{ m}$, wave period 10.0 sec.

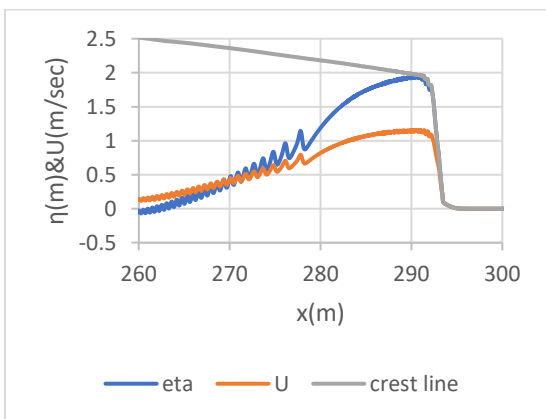


Fig (12) Wave profile at shallow water $h = 2.4\text{ m}$, wave period 8.0 sec.

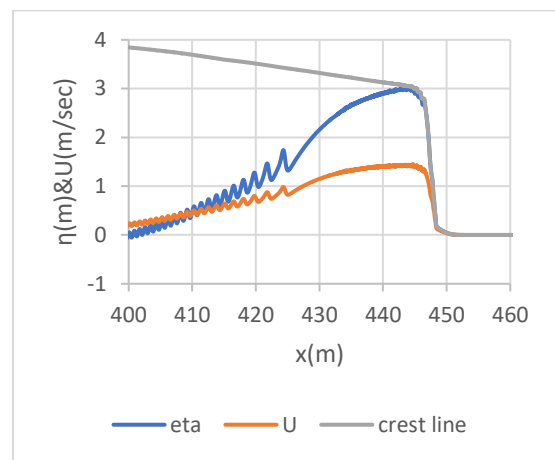


Fig (15) Wave profile at shallow water $h = 3.75\text{ m}$, wave period 10.0 sec.

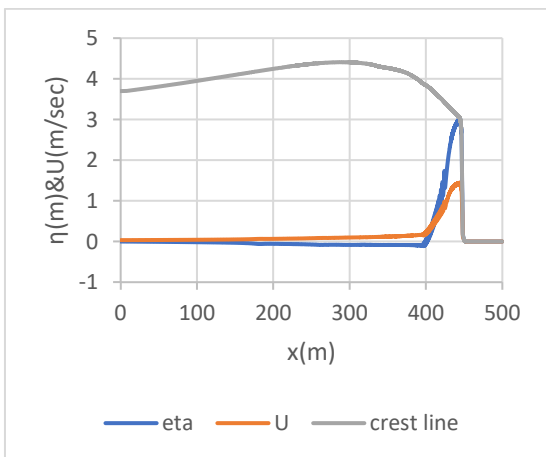


Fig (13) Shoaling-breaking, wave period 10.0 sec.

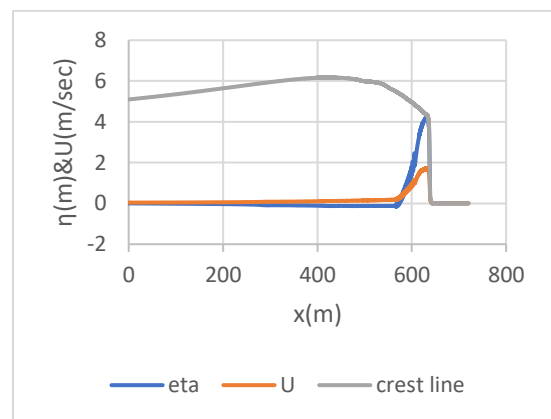


Fig (16) Shoaling-breaking, wave period 12.0 sec.

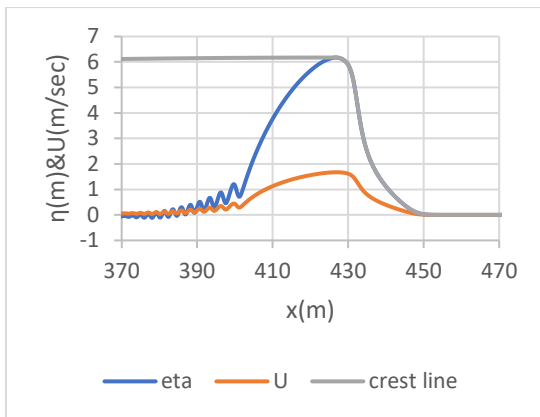


Fig (17) Wave profile around breaking point $h_b = 15.768 \text{ m}$, wave period 12.0 sec.

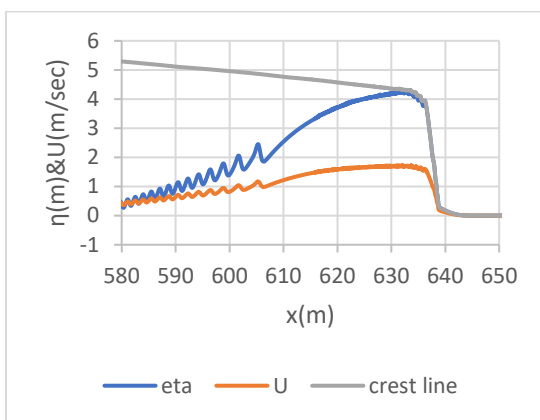


Fig (18) Wave profile at shallow water $h = 5.25 \text{ m}$, wave period 12.0 sec.

From the model execution over the sloping bottom, it was found that the model is capable of simulating shoaling and breaking processes well, where the model can pass through the breaking condition and continue into shallow water, but the model stops at water depths still far from the coastline. This indicates that further development of the energy-loss formulation is likely required.

VIII. CONCLUSION

This study shows that the original Euler momentum conservation equation contains an excessive driving force, leading to instability when applied to short waves with large amplitudes. It is suitable only for long-wave conditions with very small amplitudes. Therefore, modification of the equation is necessary.

The three modifications introduced in this work produce a formulation capable of representing the maximum wave amplitude for each wave period and generating wavelengths reasonably close to natural conditions. The momentum equilibrium equation supplies the necessary

potential energy to balance kinetic energy changes in the water-particle velocity. Its contribution is evident in the improved model stability during wave breaking, reducing oscillations in free-surface elevation and particle velocity.

Overall, the combination of the modified Euler momentum equation and the momentum equilibrium equation yields a stable and reliable time-series wave model. Further work is needed to refine the energy-loss formulation so the model can propagate into very shallow coastal waters.

REFERENCES

- [1] Boussinesq, J. (1871). Theorie de l'intumescence liquide aplee onde solitaire ou de translation se propageant dans un canal rectangulaire. *Comptes Rendus de le Academie des Sciences*. 72:755-759.
- [2] Peregrine, D.H. (1967). "Long Waves on Beach". *Journal of Fluid Mechanics*. 27.(4):815-827. Bibcode:1967 JFM (27) ...815P. doi:10.1017/S0022112067002605. S2CID119385147.
- [3] Hamm, L., Madsen, P.A., Peregrine, D.H. (1993). "Wave transformation in the nearshore zone: A review." *Coastal Engineering*. 21 (1-3):5-39. Bibcode: 1993 CoasE.21....5H. doi:10.1016/0378-3839(93)90044-9.
- [4] Nwogu, O.G. (1993). Alternative form of Boussinesq equations for nearshore wave propagation. *Journal of Waterway, Port, Coastal, and Ocean Engineering* 119, 618. [https://doi.org/10.1061/\(ASCE\)0733-950X\(1993\)119:6\(618\)](https://doi.org/10.1061/(ASCE)0733-950X(1993)119:6(618)). Google Scholar Crossref.
- [5] Dingemans, M.W. (1997). *Wave Propagation over uneven Bottoms*. Advanced Series on Ocean Engineering 13. World Scientific, Singapore. ISBN 978-981-02-0247-3. Archived from the original on 2012-02-08. Retrieved 2008-01-21. See Part 2, Chapter 5.
- [6] Johnson, R.S. (1997). *A modern introduction to the mathematical theory of water waves*. Cambridge Texts in Applied Mathematics. Vol.19. Cambridge University Press. ISBN 0-521-59832-X.
- [7] Madsen, P.A., Schaffer, H.A. (1998). Higher-order boussinesq type equations for surface gravity waves: Derivation and analysis. *Phil Trans. R. Soc.Land. A*, 356:3123-3184.
- [8] Kirby, J.T. (2003). "Boussinesq models and application to nearshore wave propagation, surfzone processes and wave-induced current ". In Laxhan, V.C. (ed). *Advances in Coastal Modeling Elsevier Oceanography Series*. Vol.67. Elsevier. pp 1-41. ISBN 0-444-51149-0.
- [9] Hutahaean, S. (2025a). Time-Series Water Wave Model based on Energy Conservation. *International Journal of Advance Engineering Research and Science (IJAERS)*. Vol. 12, Issue 10; Oct.; 2025, pp 17-29. Article DOI: <https://dx.doi.org/10.22161/ijaers.1210.2>.
- [10] Hutahaean, S. (2023). Water Wave Velocity Potential on Sloping Bottom in Water Wave Transformation Modeling. *International Journal of Advance Engineering Research and*

- Science (IJAERS). Vol. 10, Issue 10; Oct, 2023, pp 149-157.
Article DOI: <https://dx.doi.org/10.22161/ijaers.1010.15>.
- [11] Hutahaean, S. (2025b). New Weighted Taylor Series for Water Wave Energy Loss and Littoral Current Analysis. International Journal of Advance Engineering Research and Science (IJAERS). Vol. 12, Issue 1; Jan, 2025, pp 27-39. Article DOI: <https://dx.doi.org/10.22161/ijaers.121.3>.
- [12] Protter, Murray, H.; Morrey, Charles, B. Jr. (1985). Differentiation Under the Integral Sign. Intermediate Calculus (second ed.). New York: Springer pp. 421-426. ISBN 978-0-387-96058-6.
- [13] Hutahaean, S. (2025c). Enhanced Time-Series Water Wave Model through Refinement of Convective Acceleration and Driving Force in the Velocity Equation. International Journal of Advance Engineering Research and Science (IJAERS). Vol. 12, Issue 9; Sep, 2025, pp 11-19. Article DOI: <https://dx.doi.org/10.22161/ijaers.129.2>.
- [14] Dean, R.G., Dalrymple, R.A. (1991). Water wave mechanics for engineers and scientists. Advance Series on Ocean Engineering.2. Singapore: World Scientific. ISBN 978-981-02-0420-4. OCLC 22907242.
- [15] Komar, P.D. & Gaughan M.K. (1972). Airy Wave Theory and Breaker Height Prediction, Coastal Engineering Proceedings, 1 (13).
- [16] Mc Cowan, J. (1894). On the highest waves of a permanent type, Philosophical Magazine, Edinburgh 38, 5th Series, pp. 351-358.